

Lifshitz Scaling Effects on Holographic Superconductors

Jun-Wang Lu^{1,2}, Ya-Bo Wu^{1,*}, Peng Qian², Yue-Yue Zhao¹, and Xue Zhang¹

¹*Department of Physics, Liaoning Normal University, Dalian, 116029, China*

²*State Key Laboratory of Theoretical Physics, Institute of Theoretical Physics,
Chinese Academy of Sciences, Beijing 100190, China*

Via numerical and analytical methods, the effects of the Lifshitz dynamical exponent z on holographic superconductors are studied in some detail, including s wave and p wave models. Working in the probe limit, we find that the behaviors of holographic models indeed depend on concrete value of z . We obtain the condensation and conductivity in both Lifshitz black hole and soliton backgrounds with general z . For both s wave and p wave models in the black hole backgrounds, as z increases, the phase transition becomes more difficult and the growth of conductivity is suppressed. For the Lifshitz soliton backgrounds, when z increases ($z = 1, 2, 3$), the critical chemical potential decreases in the s wave cases but increases in the p wave cases. For p wave models in both Lifshitz black hole and soliton backgrounds, the anisotropy between the AC conductivity in different spatial directions is suppressed when z increases. The analytical results uphold the numerical results.

PACS numbers: 11.25.Tq, 04.70.Bw, 74.20.-z

Keywords: AdS/CFT correspondence, Holographic superconductor, Lifshitz gravity

I. INTRODUCTION

The gauge/gravity duality provides us a powerful tool to study the strong coupled field theory by means of its dual gravity description [1]. The high temperature superconductor is a promising area for its application. The holographic s wave superconductor was first realized via an Einstein-Maxwell theory coupled to a complex scalar field in the 4 dimensional Schwarzschild anti-de Sitter (AdS) black hole [2]. The condensation of the scalar breaks the U(1) symmetry of the system, mimicking conductor/superconductor phase transition. Soon after, this model has been widely studied in the literature, including numerical approach [3, 4] as well as analytical method [5]. By using the SU(2) gauge field in the bulk, a holographic p wave model was constructed in Ref. [6], in which the condensed vector field breaks the U(1) symmetry as well as spatial rotational symmetry spontaneously. Holographic p wave superconductors have also been realized by adding a charged

*E-mail address:ybwu61@163.com

vector field [7, 8] or constructed from the condensation of a two-form field [9] in the bulk. Holographic d wave models were built by introducing a charged massive spin-two field propagating in the bulk [10–12].

On the other hand, the holographic insulator/superconductor phase transition was studied in the 5 dimensional AdS soliton background coupled to a Maxwell field and a charged scalar field [13]. It was shown that when the chemical potential is beyond a critical value μ_c , the normal phase modeling the insulator with a mass gap becomes unstable and results in a new hairy solution dual to the superconductor phase at the boundary theory. Further studies based on this model can be found, for example, in Refs. [14–19]. However, for the p wave model in the soliton background, up to now, the conductivity has been discussed only in the direction perpendicular to the condensed vector [18]. To see the anisotropy, it is helpful to calculate the conductivity along the condensing direction.

Recently, phase transitions in many condensed matter systems are found to be governed by the so called Lifshitz fixed points which exhibit the anisotropic scaling of spacetime $t \rightarrow \lambda^z t, \vec{x} \rightarrow \lambda \vec{x}$ ($z \neq 1$), where z is the dynamical exponent representing the anisotropy of the spacetime. The metric dual to this scaling in the $D = d + 2$ dimensional spacetime was proposed in Ref. [20]

$$ds^2 = L^2 \left(-r^{2z} dt^2 + r^2 d\vec{x}^2 + \frac{dr^2}{r^2} \right), \quad (1)$$

where $d\vec{x}^2 = dx_1^2 + \dots + dx_d^2$ and $r \in (0, \infty)$. This geometry reduces to the AdS spacetime when $z = 1$, while it is a gravity dual with the Lifshitz scaling as $z > 1$.

The Lifshitz spacetime (1) can be constructed by a massless scalar coupled to an Abelian gauge field with the D dimensional action [21]

$$S = \frac{1}{16\pi G_{d+2}} \int d^{d+2}x \sqrt{-g} \left(R - 2\Lambda - \frac{1}{2} \partial_\mu \varphi \partial^\mu \varphi - \frac{1}{4} e^{\lambda\varphi} \mathcal{F}_{\mu\nu} \mathcal{F}^{\mu\nu} \right). \quad (2)$$

The generalization of (1) to the case with finite temperature and arbitrary $z \geq 1$ is [22]

$$ds^2 = L^2 \left(-r^{2z} f(r) dt^2 + \frac{dr^2}{r^2 f(r)} + r^2 \sum_{i=1}^d dx_i^2 \right), \quad (3)$$

where

$$f(r) = 1 - \frac{r_+^{z+d}}{r^{z+d}}, \quad \Lambda = -\frac{(z+d-1)(z+d)}{2L^2}. \quad (4)$$

The Hawking temperature of the Lifshitz black hole is

$$T = \frac{(z+d)r_+^z}{4\pi}, \quad (5)$$

where r_+ denotes the horizon. Besides, other asymptotical Lifshitz black hole solutions were also found, for example, in Refs. [23–26], based on which the holographic superconductors and transport coefficients were studied in Refs. [27–32]. For the solution (3), the Wilson loop, transport coefficients as well as the tidal force with general z were discussed in Refs. [22, 33]. For the special case $D = 4$, the investigation involves the binding energy, the drag force and the DC conductivity in Ref. [34], s (p) wave holographic superconductors with $z = 2$ in Ref. [35] as well as the connection between the thermodynamical quantities and the quasinormal frequency in Ref. [36].

In this work, we are going to study systematically the effects of general z on the holographic superconductors in the spacetime (3). We are to extend the previous works [33, 35] to the Lifshitz black holes with general z in the probe limit, including s wave and p wave models. For all cases, there exists a critical temperature T_c , which decreases when we increase z ($z = 1, 2$ in $D = 4$ and $z = 1, 2, 3$ in $D = 5$). This indicates that the increasing z inhibits the superconducting condensation. Near T_c , the condensations of both the s wave and p wave models behave as $\sim (1 - (T/T_c)^{d/z})^{1/2}$, which looks different from the standard form $\sim (1 - T/T_c)^{1/2}$. This results from the Lifshitz scaling dimension. In this sense we say the critical exponent for the condensation is still $1/2$. In addition, for p wave cases, the anisotropy between the AC conductivity in y direction σ_{yy} and in x direction σ_{xx} seems to be suppressed as z increases. Furthermore, we shall generalize the works [13, 18, 37] to the AdS Lifshitz soliton backgrounds. With the increasing z ($z = 1, 2, 3$), the critical chemical potential μ_c decreases in s wave models while increases in p wave cases. Especially, we calculate the conductivity along the condensing direction in p wave models, which indicates that the increasing z might also suppress the anisotropy between σ_{yy} and σ_{xx} . All above results show that the behaviors of holographic models indeed depend on concrete value of z .

This paper is organized as follows. In section II, we investigate the s wave superconductors in the Lifshitz black hole and soliton backgrounds with general z and D numerically and analytically. By using the same method, p wave models are studied in Sec. III. The final section is devoted to the conclusions and the further discussions.

II. HOLOGRAPHIC S WAVE SUPERCONDUCTORS IN LIFSHITZ SPACETIMES

In this section, we firstly discuss the holographic s wave superconductors in the Lifshitz black holes numerically. To complement the numerical results, we also study these models by the Sturm-Liouville (SL) variational method. In the second part of this section, by virtue of the similar methods, we will consider the holographic s wave superconductor model in the Lifshitz soliton

background.

Following Refs. [2, 13], the holographic s wave superconductor can be built in the Lifshitz gravity coupled to a Maxwell field and a complex scalar field with the Lagrangian density

$$L_m = -\frac{1}{4}F_{\mu\nu}F^{\mu\nu} - |D_\mu\psi|^2 - m^2|\psi|^2, \quad (6)$$

where $D_\mu = \nabla_\mu - iqA_\mu$, $F_{\mu\nu} = \nabla_\mu A_\nu - \nabla_\nu A_\mu$ and m (q) is the mass (charge) of the scalar field ψ . By using the Euler-Lagrange equation, the equations of motion of ψ and A_ν read

$$D_\mu D^\mu \psi - m^2 \psi = 0, \quad (7)$$

$$\nabla^\mu F_{\mu\nu} - iq(\psi^* D_\nu \psi - \psi D_\nu^* \psi^*) = 0. \quad (8)$$

As usual, we take the scalar field and the gauge field to be $\psi = \psi(r)$ and $A_\mu dx^\mu = \phi(r)dt$, respectively.

A. s wave superconductors in Lifshitz black holes

Now, let us consider the s wave superconductor in the black hole background. Plugging the Lifshitz metric (3) into Eqs. (7) and (8), we can obtain

$$\psi'' + \left(\frac{d+z+1}{r} + \frac{f'}{f} \right) \psi' + \frac{q^2 \phi^2}{r^{2z+2} f^2} \psi - \frac{m^2 L^2}{r^2 f} \psi = 0, \quad (9)$$

$$\phi'' + \frac{d-z+1}{r} \phi' - \frac{2q^2 L^2 \psi^2}{r^2 f} \phi = 0. \quad (10)$$

Concretely, we focus our numerical calculation on the cases of $z = 1, 2$ in $D = 4$ and $z = 1, 2, 3$ in $D = 5$. For simplicity, we scale $L = 1, q = 1$. At the horizon, we impose $\phi(r_+) = 0$ to satisfy the finite norm of A_μ , while $\psi(r_+)$ needs to be regular. Near the boundary $r \rightarrow \infty$, $\psi(r)$ and $\phi(r)$ behave as

$$\psi(r) = \frac{\psi_1}{r^{\Delta_-}} + \frac{\psi_2}{r^{\Delta_+}} + \dots, \quad (11)$$

$$\phi(r) = \mu - \frac{\rho}{r^{d-z}} + \dots (z < d), \text{ and } \mu - \rho \ln \xi r + \dots (z = d), \quad (12)$$

with $\Delta_\pm = \frac{z+d \pm \sqrt{(z+d)^2 + 4m^2}}{2}$ and ξ a constant. ψ_1 (ψ_2) is usually regarded as the source (the expectation value) of the dual operator \mathcal{O} . To guarantee the spontaneous breaking of the U(1) symmetry, we impose $\psi_1 = 0$. We denote $\Delta = \Delta_+$ throughout the paper. Following the AdS/CFT dictionary, μ (ρ) is interpreted as chemical potential (charge density) in the dual field theory. m^2 has a lower bound as $m^2 = -(z+d)^2/4$ with $\Delta = \Delta_{BF} = (z+d)/2$. In that case, there is a

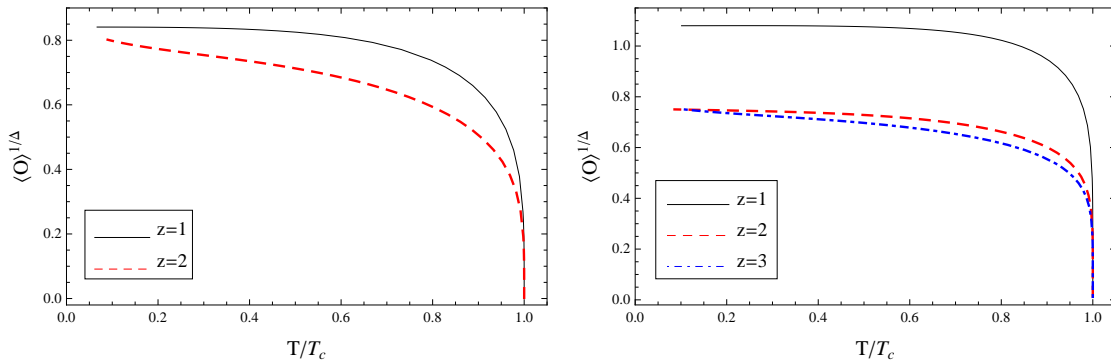


FIG. 1: The condensation versus temperature of the s wave models for $\Delta = 2$ in $D = 4$ (left) and $\Delta = 3$ in $D = 5$ (right). Curves from top to bottom correspond to $z = 1$ (solid), 2(dashed), 3(dotdashed), respectively.

logarithmic term in the asymptotical expansion. We treat such a term as the source set to be zero to avoid the instability induced by this term [3]. In this paper we consider the canonical ensemble where ρ is fixed.

Figure 1 shows the condensation as a function of temperature for various z . The critical temperature T_c and related fitting results are listed in Tab. I. Previous studies for $z = 1$ [2, 3] are also included for comparison. From the figure and the results in the table, we can find that the properties of the system depend on z . In all cases, there is a critical temperature T_c . When we increase z ($z = 2$ and $z = 3$), T_c decreases for fixed Δ , which might suggest that the larger z is, the more difficult the phase transition becomes. On the other hand, all curves have a square root behavior near T_c , which is expected from the mean field theory.

To compute the AC conductivity at the boundary, we need to study the perturbation of the gauge field in the superconducting phase. Due to the rotational symmetry of the s wave superconductor, without loss of generality, we turn on the perturbation along the x direction with the ansatz $\delta A_\mu = A_x(r)e^{-i\omega t}$. The linearized equation of the perturbation is

$$A_x'' + \left(\frac{d+z-1}{r} + \frac{f'}{f} \right) A_x' + \frac{\omega^2}{r^{2z+2}f^2} A_x - \frac{2\psi^2}{r^2 f} A_x = 0. \quad (13)$$

At the horizon, the perturbation is imposed to satisfy the ingoing wave condition

$$A_x(r) = (r - r_+)^{-i\omega/4\pi T} (1 + A_{x1}(r - r_+) + A_{x2}(r - r_+)^2 + A_{x3}(r - r_+)^3 + \dots). \quad (14)$$

And at the boundary, the asymptotical expansion of $A_x(r)$ is of the form

$$A_x(r) = A^{(0)} + \frac{A^{(d+z-2)}}{r^{d+z-2}} + \dots. \quad (15)$$

The case of $z = 1, d = 3$ is a little more different. A logarithmic term $\frac{A^{(0)}\omega^2}{2r^2} \ln \xi r$ should be added to the formula (15), where ξ is a constant. According to the Kubo formula, the AC conductivity

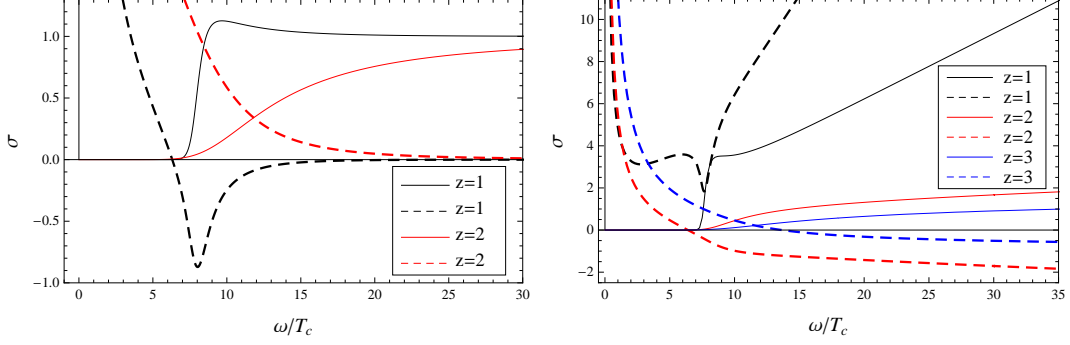


FIG. 2: The real (solid) and imaginary (dashed) part of the AC conductivity versus frequency of the s wave model at $T/T_c \approx 0.1$ with $\Delta = 2$, $z = 1$ (black), 2 (red) in $D = 4$ (left), and $\Delta = 3$, $z = 1$ (black), 2 (red), 3 (blue) in $D = 5$ (right).

reads

$$\sigma(\omega) = \frac{-1}{i\omega} \lim_{r \rightarrow \infty} r^{d+z-1} \frac{A'_x}{A_x}. \quad (16)$$

In the case of $z = 1$ in $D = 5$, a logarithmic divergence exists in $\sigma(\omega)$, which can be canceled by the holographic renormalization. The frequency dependent conductivity is plotted in Fig. 2, from which we have some comments as follows.

- (1) At $\omega \approx 0$, there exists a pole for the imaginary part in $D = 4$ (5). This pole corresponds to a delta function in the real part, which means the DC superconductivity.
- (2) When $z = 1$ in $D = 4$ (5), there exists an obvious gap frequency ω_g satisfying $\omega_g/T_c \approx 8$, which reduces to the results in Refs. [2, 3]. When $z = 2$ (3) in $D = 5$, the gap of the real part becomes blurred and the imaginary part does not exhibit a minimum but rather decreases monotonously with the increase of frequency. The behavior of the conductivity with $z = 2$ in $D = 4$ is similar to that in the case of $z \neq 1$ in $D = 5$. Especially, the results corresponding to $m^2 = -3$ (0) can recover the ones in Ref. [35].

Usually, superfluid density n_s can be expressed as the coefficient of $Im[\sigma]$ at zero frequency limit, i.e., $n_s \approx \lim_{\omega \rightarrow 0} \omega Im[\sigma]$. In the left plot of Fig. 3, we typically show n_s with different z at $\Delta = 3$ in $D = 5$ and list the coefficient of n_s near T_c in Tab. I. It follows that n_s near the critical temperature decreases with $(1 - T/T_c)$ linearly. Besides, the other important quantity is the contribution of the normal component to DC conductivity $n_n = \lim_{\omega \rightarrow 0} Re[\sigma]$ which is found to decrease as $n_n \approx e^{-\tilde{\Delta}/T}$, where $\tilde{\Delta}$ is interpreted as the mass of excited quasi-particles about the fermi surface. $\tilde{\Delta}$ is listed in Tab. I, from which we find that for fixed Δ , $\tilde{\Delta}$ decreases when we increases z ($z = 2, 3$).

TABLE I: The results of s wave superconductors in the 4 (5) dimensional Lifshitz black holes, where $t = 1 - T/T_c$, $\tilde{t} = 1 - (T/T_c)^{1/2}$, $\tilde{\Delta}$ denotes the mass of the excited quasi-particles about the fermi surface and the subscript $_{SL}$ denotes the quantity calculated by the SL method.

D	z	m^2	Δ	$T_c/\rho^{z/d}$	$\langle \mathcal{O} \rangle^{1/\Delta}(T \approx T_c)$	$n_s(T \approx T_c)$	$\tilde{\Delta}$	$T_{c;SL}/\rho^{z/d}$	$\langle \mathcal{O} \rangle_{SL}^{1/\Delta}(T \approx T_c)$
4	1	-2	2	0.118	$1.19t^{1/2\Delta}$	$2.82t$	0.48	0.117	$0.95t^{1/2\Delta}$
4	1	-5/4	5/2	0.099	$1.06t^{1/2\Delta}$	$2.43t$	0.16	0.097	$0.80t^{1/2\Delta}$
4	2	-4	2	0.068	$0.92t^{1/2\Delta}$	$1.95t$	0.17	—	—
4	2	-15/4	5/2	0.047	$0.76t^{1/2\Delta}$	$1.25t$	0.08	—	—
4	2	-3	3	0.035	$0.66t^{1/2\Delta}$	$0.88t$	0.02	—	—
4	2	0	4	0.013	$0.31t^{1/2\Delta}$	$0.50t$	—	—	—
5	1	-15/4	5/2	0.220	$1.56t^{1/2\Delta}$	$5.19t$	1.98	0.218	$1.36t^{1/2\Delta}$
5	1	-3	3	0.197	$1.44t^{1/2\Delta}$	$4.49t$	1.10	0.196	$1.22t^{1/2\Delta}$
5	1	-7/4	7/2	0.182	$1.36t^{1/2\Delta}$	$3.87t$	0.44	0.180	$1.10t^{1/2\Delta}$
5	1	0	4	0.171	$1.30t^{1/2\Delta}$	$3.38t$	—	0.168	$1.01t^{1/2\Delta}$
5	2	-6	3	0.087	$1.00\tilde{t}^{1/2\Delta}$	$1.53t$	0.28	0.087	$0.94\tilde{t}^{1/2\Delta}$
5	2	-21/4	7/2	0.074	$0.91\tilde{t}^{1/2\Delta}$	$1.12t$	0.17	0.074	$0.85\tilde{t}^{1/2\Delta}$
5	2	-4	4	0.064	$0.80\tilde{t}^{1/2\Delta}$	$0.86t$	0.08	0.064	$0.77\tilde{t}^{1/2\Delta}$
5	3	-9	3	0.045	$0.82t^{1/2\Delta}$	$0.93t$	0.11	—	—
5	3	-35/4	7/2	0.035	$0.75t^{1/2\Delta}$	$0.57t$	0.06	—	—
5	3	-8	4	0.028	$0.68t^{1/2\Delta}$	$0.40t$	0.04	—	—

Next, we study the critical behavior of the s wave superconductors by using the SL eigenvalue method [5]. For simplicity, we consider the cases of $1 \leq z < d$. Taking $u = r_+/r$, Eqs. (9) and (10) can be rewritten as

$$\psi'' + \frac{u^{d+z} + d + z - 1}{u(u^{d+z} - 1)}\psi' + \frac{m^2(u^{d+z} - 1) + r_+^{-2z}u^{2z}\phi^2}{u^2(u^{d+z} - 1)^2}\psi = 0, \quad (17)$$

$$\phi'' + \frac{z - d + 1}{u}\phi' + \frac{2\psi^2}{u^2(u^{d+z} - 1)}\phi = 0. \quad (18)$$

When $T \rightarrow T_c$, the scalar field vanishes, so the solution of $\phi(u)$ is

$$\phi(u) = \lambda r_{+c}^z (1 - u^{d-z}), \lambda = \frac{\rho}{r_{+c}^d}, \quad (19)$$

where we have considered $\phi(1) = 0$. We define a new function $F(u)$ by

$$\psi(u) = \frac{\langle \mathcal{O} \rangle}{r_{+c}^{\Delta}} u^{\Delta} F(u). \quad (20)$$

Without loss of generality, we concentrate on the case of $D = 5$. Substituting Eqs. (19) and (20),

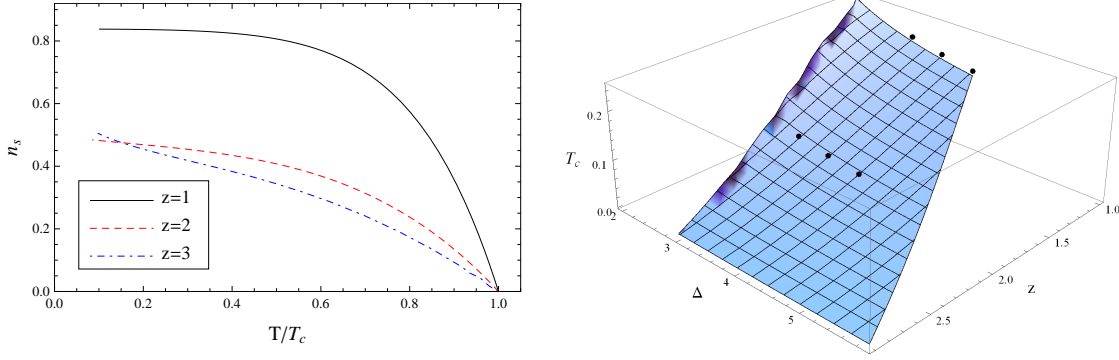


FIG. 3: The superfluid density versus temperature (left) with $\Delta = 3$, $z = 1, 2, 3$ (from top to bottom) and critical temperature T_c versus z and Δ (right) of the s wave models in the 5 dimensional black holes. The special points in the right plot correspond to the cases of the above numerical results with $z = 1, 2$.

we can reduce Eq. (17) to the SL eigenvalue equation

$$\frac{d}{du}(\mathcal{T}F') - \mathcal{P}F + \lambda^2 \mathcal{Q}F = 0, \quad (21)$$

where coefficients $\mathcal{T}, \mathcal{P}, \mathcal{Q}$ are listed as follows

$$\begin{aligned} \mathcal{T} &= (1 - u^{z+3}) u^{\sqrt{4m^2 + z^2 + 6z + 9} + 1}, \\ \mathcal{P} &= \frac{1}{2} \left((z + 3) \left(\sqrt{4m^2 + (z + 3)^2} + z + 3 \right) + 2m^2 \right) u^{\sqrt{4m^2 + (z+3)^2} + z + 2}, \\ \mathcal{Q} &= -\frac{u^{2z} (u^3 - u^z)^2 u^{\sqrt{4m^2 + (z+3)^2} - 2z - 1}}{u^{z+3} - 1}. \end{aligned} \quad (22)$$

According to the boundary conditions for $F(u)$, i.e., $F(0) = 1$ and $F'(0) = 0$, we can introduce a trial function

$$F = F_\alpha(u) \equiv 1 - \alpha u^2. \quad (23)$$

The eigenvalue λ^2 should minimize the expression with respect to the coefficient α

$$\lambda^2 = \frac{\int_0^1 du (\mathcal{T}F'^2 - \mathcal{P}F^2)}{\int_0^1 du \mathcal{Q}F^2}. \quad (24)$$

We show the critical temperature depending on both Δ and z in the right plot of Fig. 3, in which some cases discussed in Refs. [2, 3, 5] are also included for comparison. For fixed Δ , T_c decreases smoothly when one increases z ($1 \leq z < 3$). Especially, the analytical critical temperature $T_{c,SL}$ listed in Tab. I is consistent with the numerical result. The results in $D = 4$ are similar to the cases in $D = 5$.

When the temperature is slightly below T_c , the parameter $\frac{\langle \mathcal{O} \rangle^2}{r_+^{2\Delta}}$ is very small, so we can expand $\phi(u)$ in the form

$$\frac{\phi(u)}{r_+^z} = \lambda(1 - u^{3-z}) + \frac{\langle \mathcal{O} \rangle^2}{r_+^{2\Delta}} \chi(u) + \dots \quad (25)$$

The equation of $\chi(u)$ reduces to

$$\chi'' + \frac{z-2}{u}\chi' - \frac{2\lambda(\alpha u^2 - 1)^2(u^3 - u^z)u\sqrt{4m^2 + (z+3)^2 + 1}}{u^{z+3} - 1} = 0. \quad (26)$$

Considering conditions $\chi(1) = 0$ and $\chi'(1) = 0$, we can read off

$$u^{z-2}\chi(u)|_{u \rightarrow 0} = 2\lambda \int_1^0 du \frac{(\alpha u^2 - 1)^2(u^3 - u^z)u\sqrt{4m^2 + (z+3)^2 + z-1}}{u^{z+3} - 1}. \quad (27)$$

Expanding $\chi(u)$ near the boundary $u \rightarrow 0$, we can obtain

$$\frac{\rho}{r_+^3 \lambda} - 1 = -\frac{\langle \mathcal{O} \rangle^2}{r_+^{2\Delta}} \frac{\chi^{3-z}(0)}{\lambda(3-z)!}, \quad (28)$$

by comparing the coefficient of u^{3-z} in Eq. (25) with the one in Eq. (12). Note that here z is limited to be an integer, i.e., $z = 1, 2$. Combining $r_{+c} = (\rho/\lambda)^{1/3}$ with the temperature (5), we have

$$\langle \mathcal{O} \rangle^{\frac{1}{\Delta}} = \left(\frac{4\pi T}{3+z} \right)^{\frac{1}{z}} \left(\frac{\lambda(3-z)!}{-\chi^{(3-z)}(0)} \right)^{\frac{1}{2\Delta}} \left(1 - \left(\frac{T}{T_c} \right)^{\frac{3}{z}} \right)^{\frac{1}{2\Delta}}. \quad (29)$$

We list the coefficient of the condensation near T_c in Tab. I, from which we find the result agrees with the numerical result at the same order and the critical exponent $\frac{1}{2}$ exists in the superconducting system. It should be pointed that the critical behavior $\langle \mathcal{O} \rangle \sim (1 - (T/T_c)^{d/z})^{1/2}$ looks a little different from the standard form $\sim (1 - T/T_c)^{1/2}$. This is due to the scaling dimension in the Lifshitz case: $r \rightarrow \lambda r, T \rightarrow \lambda^z T, \langle \mathcal{O} \rangle \rightarrow \lambda^\Delta \langle \mathcal{O} \rangle, \rho \rightarrow \lambda^d \rho$. It is in this sense $\langle \mathcal{O} \rangle \sim (1 - (T/T_c)^{d/z})^{1/2}$ that we say the critical exponent for the condensation is $\frac{1}{2}$.

B. s wave superconductors in Lifshitz solitons

In this subsection we consider the insulator/superconductor phase transition by generalizing the study in Ref. [13] to the Lifshitz soliton background with general z . By performing the double Wick rotation [37] to the black hole solution (3), a $(d+2)$ dimensional AdS Lifshitz soliton can be obtained

$$ds^2 = L^2 \left(-r^2 dt^2 + \frac{dr^2}{r^2 f(r)} + r^2 \sum_{i=1}^{d-1} dx_i^2 + r^{2z} f(r) d\chi^2 \right), \quad (30)$$

where $f(r)$ still takes the formula (4). To distinguish the soliton from the black hole, we denote the tip of the soliton geometry by r_0 . The Scherk-Schwarz period should be imposed along the direction χ to ensure the geometry smooth. Due to the compactness of the spatial direction, this $(d+2)$ dimensional soliton geometry is dual to a d dimensional field theory.

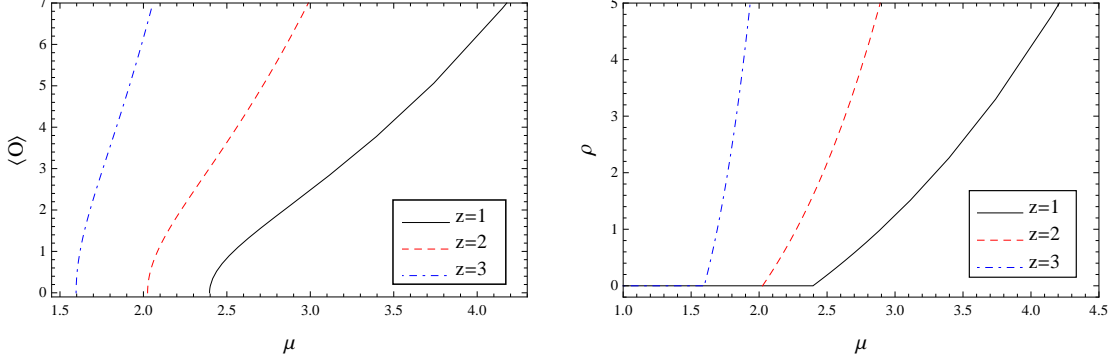


FIG. 4: The condensation (left) and the charge density (right) versus chemical potential of the s wave superconductor with $\Delta = 3$ and $z = 1, 2, 3$ (from right to left) in the 5 dimensional solitons.

When we take into account the action (6) and the ansatz $A_t = \phi(r)$ and $\psi = \psi(r)$ [13] in the background (30), the equations of motion for ψ and ϕ read

$$\psi'' + \left(\frac{d+z+1}{r} + \frac{f'}{f} \right) \psi' + \frac{q^2 \phi^2}{r^4 f} \psi - \frac{m^2 L^2}{r^2 f} \psi = 0, \quad (31)$$

$$\phi'' + \left(\frac{d+z-1}{r} + \frac{f'}{f} \right) \phi' - \frac{2q^2 L^2 \psi^2}{r^2 f} \phi = 0, \quad (32)$$

which implies that the behavior of superconductors is determined by $(d+z)$ and m^2 . We impose the Neumann-like boundary condition [13] to make both $\psi(r_0)$ and $\phi(r_0)$ finite at the tip $r = r_0$. Near the boundary $r \rightarrow \infty$, $\psi(r)$ obeys the form (11), while $\phi(r)$ is

$$\phi(r) = \mu - \frac{\rho}{r^{d+z-2}} + \dots, \quad (33)$$

where the coefficients μ and ρ are interpreted as the chemical potential and the charge density in the boundary field theory, respectively. We still scale $L = 1, q = 1$ for simplicity. Note that we consider the cases of $z \geq 1$ in $D = 4$ (5). Typically, taking the integer $z = 1, 2, 3$, we plot the condensation and ρ in Fig. 4, and list the critical chemical potential μ_c as well as related fitted results in Tab. II, from which we can conclude the following results: for fixed Δ , μ_c decreases when we increase z ($z = 2$ and $z = 3$); and when μ is slightly beyond μ_c , $\rho \sim (\mu - \mu_c)$ while $\langle \mathcal{O} \rangle \sim \sqrt{\mu - \mu_c}$, which might indicate the system suffers a second order phase transition. As $z = 1$ and $m^2 = -15/4$ in $D = 5$, μ_c reduces to the result obtained in Ref. [13].

To calculate the conductivity, we turn on the perturbation $\delta A = A_x(r)e^{-i\omega t}$, which results in the linearized equation of motion

$$A_x'' + \left(\frac{d+z-1}{r} + \frac{f'}{f} \right) A_x' + \frac{\omega^2}{r^4 f} A_x - \frac{2\psi^2}{r^2 f} A_x = 0. \quad (34)$$

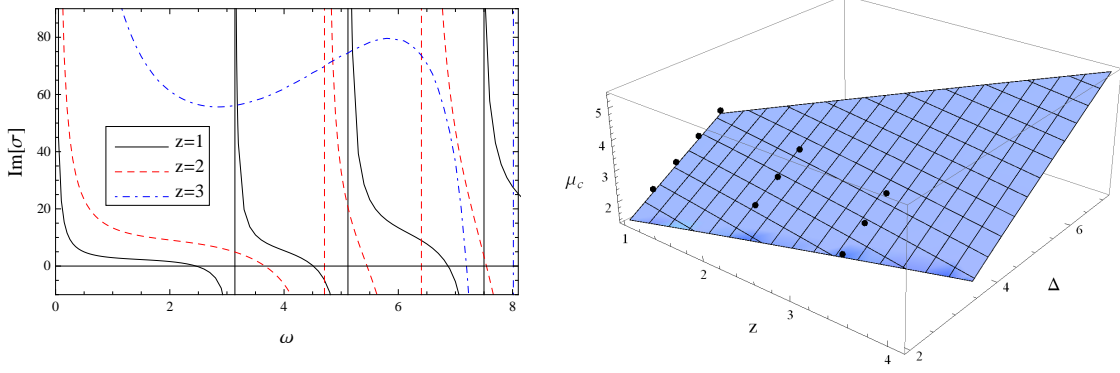


FIG. 5: The conductivity versus frequency with $\Delta = 3$ and $z = 1, 2, 3$ (from bottom to top) at $\mu/\mu_c \approx 1.74$ (left) and the analytical μ_c as a function of Δ and z (right) of the s wave models in the 5 dimensional solitons. The special points in the right plot correspond to the results of the above numerical calculation.

In order for A_x to be finite at the tip, we take the ansatz of A_x near the tip

$$A_x(r) = 1 + A_{s1}(r - r_0) + A_{s2}(r - r_0)^2 + A_{s3}(r - r_0)^3 + \dots \quad (35)$$

Near the boundary $r \rightarrow \infty$, the general falloff of A_x behaves as

$$A_x(r) = \begin{cases} A^{(0)} + \frac{A^{(1)}}{r} + \dots, & z = 1, d = 2, \\ A^{(0)} + \frac{A^{(2)}}{r^2} + \frac{A^{(0)}\omega^2}{2r^2} \ln \xi r + \dots, & z = 2 (1), d = 2 (3), \\ A^{(0)} + \frac{A^{(0)}\omega^2}{2r^2} + \frac{A^{(3)}}{r^3} + \dots, & z = 3 (2), d = 2 (3), \\ A^{(0)} + \frac{A^{(0)}\omega^2}{4r^2} + \frac{A^{(4)}}{r^4} + \frac{A^{(0)}\omega^4}{16r^4} \ln \xi r + \dots, & z = 3, d = 3, \end{cases} \quad (36)$$

with a constant ξ . As the conductivity in $D = 4$ is similar to the case in $D = 5$, we typically plot the conductivity in the case of $D = 5$ in the left plot of Fig. 5 and list the location of the second pole of conductivity in normal phase ω_n as well as the superfluid density n_s in Tab. II, from which we can find that as we increase z ($z = 1, 2, 3$), the location of ω_n increases while the location of the second pole of the AC conductivity in the superconducting phase ω_s moves right by comparing with its ω_n . Meanwhile the coefficient of superfluid density near μ_c increases when z increases. Results corresponding to $z = 1$ (such as μ_c , n_s and ω_n) can reduce to ones in Refs. [13, 15].

Now, we turn to the analytical calculation of the s wave models in $D = 5$. In the normal phase, the general solution $\phi(r)$ of Eq. (32) is

$$\phi(u) = C_1 \left(\frac{1}{2u^2} - \frac{{}_2F_1\left(1, -\frac{2}{d+z}; 1 - \frac{2}{d+z}; u^{d+z}\right)}{2u^2} \right) + C_2, \quad (37)$$

where ${}_2F_1$ is the hypergeometric function and $u = r_0/r$. According to the boundary conditions as ones in Refs. [13, 16, 17], we obtain $C_1 = 0$ and $C_2 = \mu$ near the tip $u = 1$. Comparing the solution

TABLE II: The numerical and analytical results of the s wave superconductors in the 4 (5) dimensional solitons, where $t = (\mu - \mu_c)^{1/2}$ and the subscript $_{SL}$ denotes the quantity calculated by the SL method. All the quantities except μ_c , ω_n and $\mu_{c;SL}$ are calculated near μ_c .

D	z	m^2	Δ	μ_c	$\langle \mathcal{O} \rangle$	ρ	n_s	ω_n	$\mu_{c;SL}$	$\langle \mathcal{O} \rangle_{SL}$	ρ_{SL}
4	1	-2	2	1.718	1.31t	1.42t ²	0.48μ _c t ²	1.49	1.719	1.09t	1.05t ²
4	1	-5/4	5/2	2.221	1.33t	1.24t ²	0.25μ _c t ²	1.49	2.221	1.10t	0.95t ²
4	1	0	3	2.722	1.36t	1.13t ²	0.15μ _c t ²	1.49	2.722	1.11t	0.89t ²
4	2	-15/4	5/2	1.888	2.48t	2.24t ²	1.26μ _c t ²	2.27	1.890	1.80t	1.33t ²
4	2	-3	3	2.396	2.50t	1.80t ²	0.63μ _c t ²	2.27	2.399	1.82t	1.15t ²
4	3	-25/4	5/2	1.497	4.28t	6.11t ²	7.67μ _c t ²	2.97	1.500	2.60t	2.27t ²
4	3	-6	3	2.024	3.97t	3.85t ²	2.56μ _c t ²	2.97	2.029	2.58t	1.71t ²
4	3	-21/4	7/2	2.540	3.97t	2.94t ²	1.23μ _c t ²	2.97	2.545	2.62t	1.42t ²
5	1	-15/4	5/2	1.888	2.47t	2.24t ²	1.25μ _c t ²	2.25	1.890	1.80t	1.33t ²
5	1	-3	3	2.396	2.49t	1.97t ²	0.62μ _c t ²	2.25	2.398	1.82t	1.15t ²
5	1	-7/4	7/2	2.901	2.58t	1.57t ²	0.37μ _c t ²	2.25	2.903	1.86t	1.03t ²
5	1	0	4	3.404	2.70t	1.38t ²	0.24μ _c t ²	2.25	3.407	1.91t	0.95t ²
5	2	-6	3	2.025	3.97t	3.51t ²	2.56μ _c t ²	2.97	2.029	2.58t	1.71t ²
5	2	-21/4	7/2	2.540	3.97t	2.64t ²	1.23μ _c t ²	2.97	2.545	2.62t	1.42t ²
5	2	-4	4	3.050	4.09t	2.20t ²	0.70μ _c t ²	2.97	3.055	2.68t	1.24t ²
5	3	-9	3	1.597	6.37t	10.80t ²	14.38μ _c t ²	3.63	1.601	3.49t	3.01t ²
5	3	-35/4	7/2	2.137	5.89t	5.39t ²	4.79μ _c t ²	3.63	2.143	3.45t	2.18t ²
5	3	-8	4	2.661	5.85t	3.84t ²	2.47μ _c t ²	3.63	2.688	3.49t	1.76t ²

at the infinity with Eq. (33), we can obtain $\rho = 0$ which is consistent with the above numerical results.

When μ is slightly beyond μ_c , the condensation can be taken as $\psi \approx \langle \mathcal{O} \rangle u^\Delta F(u)$, so the equation of F reduces to the eigenvalue equation

$$\frac{d}{du}(\mathcal{T}F') - \mathcal{P}F + \mu_c^2 \mathcal{Q}F = 0, \quad (38)$$

where coefficients $\mathcal{T}, \mathcal{P}, \mathcal{Q}$ are as follows

$$\begin{aligned} \mathcal{T} &= \left(1 - u^{d+z}\right) u^{\sqrt{(d+z)^2 + 4m^2} + 1}, \\ \mathcal{P} &= \frac{1}{2} \left((d+z)^2 + (d+z)\sqrt{(d+z)^2 + 4m^2} + 2m^2 \right) u^{\sqrt{(d+z)^2 + 4m^2} + d+z-1}, \\ \mathcal{Q} &= u^{\sqrt{(d+z)^2 + 4m^2} + 1}. \end{aligned} \quad (39)$$

By taking the trial function (23), the eigenvalue of μ_c^2 should minimize the expression (24). We

show the behavior of μ_c versus both Δ and z in the case of $D = 5$ in the right plot of Fig. 5. Some special μ_c are signed in the figure and the concrete results are listed in Tab. II. It follows that for fixed Δ , μ_c decreases smoothly with the increasing z , which is consistent with above numerical result. The results in $D = 4$ are similar to ones in $D = 5$.

When μ is away from (but very close to) μ_c , the parameter $\langle \mathcal{O} \rangle^2$ is very small, so we can expand $\phi(u)$ as

$$\phi(u) = \mu_c + \langle \mathcal{O} \rangle^2 \chi(u) + \dots . \quad (40)$$

Via the approximation $\psi \approx \langle \mathcal{O} \rangle u^\Delta F(u)$, the equation of $\chi(u)$ reads

$$\chi'' + \frac{(3u^{d+z} + d + z - 3)}{u(u^{d+z} - 1)} \chi' + \frac{2\mu_c (\alpha u^2 - 1)^2 u^{\sqrt{(d+z)^2 + 4m^2} + d + z - 2}}{u^{d+z} - 1} = 0. \quad (41)$$

By means of $T(u) = u^{-d-z+3} (1 - u^{d+z})$, Eq. (41) can be rewritten as

$$(T\chi')' - 2\mu_c (\alpha u^2 - 1)^2 u^{\sqrt{(d+z)^2 + 4m^2} + 1} = 0. \quad (42)$$

Near the boundary $u \rightarrow 0$, $\phi(u)$ can be further expanded as [16]

$$\phi(u) = \mu - \rho u^{d+z-2} \sim \mu_c + \langle \mathcal{O} \rangle^2 \left(\chi(0) + \chi'(0)u + \frac{1}{2}\chi''(0)u^2 + \frac{1}{6}\chi'''(0)u^3 + \dots \right). \quad (43)$$

Considering the constant term and the coefficients of u^{d+z-2} term in both sides of above formula respectively, we can obtain

$$\mu = \mu_c + \langle \mathcal{O} \rangle^2 \chi(0) \approx \mu_c + 2\mu_c \langle \mathcal{O} \rangle^2 \int_1^0 \frac{dy}{T(y)} \int_1^y du (\alpha u^2 - 1)^2 u^{\sqrt{(d+z)^2 + 4m^2} + 1}, \quad (44)$$

$$\rho = \frac{\chi^{(d+z-2)}(0)}{(d+z-2)!} \langle \mathcal{O} \rangle^2 \approx \frac{2\mu_c \langle \mathcal{O} \rangle^2}{d+z-2} \int_1^0 du (\alpha u^2 - 1)^2 u^{\sqrt{(d+z)^2 + 4m^2} + 1}, \quad (45)$$

where we have used $\chi(1) = 0$ as ones in Refs. [16, 17] and limited z to be integer. Concrete values of the condensation and the charge density are listed in Tab. II, which matches the above numerical results at the same order. Clearly, the results corresponding to $m^2 = -15/4$ and $z = 1$ in $D = 5$ can reduce to the ones in Refs. [13, 16].

III. HOLOGRAPHIC P WAVE SUPERCONDUCTORS IN LIFSHITZ SPACETIMES

In this section, we first study the p wave superconductor in the D dimensional Lifshitz black hole by numerical and analytical methods and then discuss the p wave model in the Lifshitz soliton

background. Along the line of proposals [6, 18], we construct the p wave superconductor via the SU(2) gauge field with the Lagrangian density

$$L_m = -\frac{1}{4}F_{\mu\nu}^a F^{a\mu\nu}, \quad (46)$$

where $F_{\mu\nu}^a$ is the field strength of the gauge field. The SU(2) group has three generators τ^i which satisfy the commutation relation $[\tau^i, \tau^j] = \epsilon^{ijk}\tau^k$ ($i, j = 1, 2, 3$). In this model, a U(1) subgroup generated by τ^3 is treated as the gauge group of electromagnetism. A gauge boson generated by τ^1 charged by this U(1) is regarded as the vector field. According to the AdS/CFT dictionary, the sub-leading term of this vector field gives the expectation value of dual vector operator J_μ . The emergence of non-trivial vector “hair” breaks the U(1) symmetry and the rotational symmetry which mimics the p wave superconducting phase transition in the condensed matter system.

Following [6, 18], we take the ansatz

$$A = \phi(r)\tau^3 dt + \psi(r)\tau^1 dx. \quad (47)$$

The equation of motion of the gauge field reads

$$\nabla_\mu F^{a\mu\nu} + \epsilon^{abc} A_\mu^b F^{c\mu\nu} = 0. \quad (48)$$

A. p wave superconductors in Lifshitz black holes

In the Lifshitz black hole background (3), the equations of motion in terms of $\phi(r)$ and $\psi(r)$ read

$$\psi'' + \left(\frac{d+z-1}{r} + \frac{f'}{f} \right) \psi' + \frac{\phi^2}{r^{2z+2} f^2} \psi = 0, \quad (49)$$

$$\phi'' + \frac{d-z+1}{r} \phi' - \frac{\psi^2}{r^4 f} \phi = 0. \quad (50)$$

As for in the s wave model, we still limit our consideration to cases $1 \leq z \leq d$ for $d = 2, 3$. At the horizon, we require $\psi(r_+)$ to be regular and $\phi(r_+) = 0$. Near the boundary, $\psi(r)$ behaves as

$$\psi(r) = \psi_0 + \frac{\langle J_x \rangle}{r^{d+z-2}} + \dots, \quad (51)$$

while $\phi(r)$ takes the form (12). As examples, we will take z as integers for concrete calculations.

We exhibit various condensation behaviors in Fig. 6 and list the related results in Tab. IV. It follows that when z increases ($z = 1, 2$ in $D = 4$ and $z = 1, 2, 3$ in $D = 5$), T_c decreases, which implies that the increasing z inhibits the phase transition. For all cases, near the critical temperature, $\langle J_x \rangle \sim (1 - (T/T_c)^{d/z})^{1/2}$, which is consistent with the result in the mean field theory.

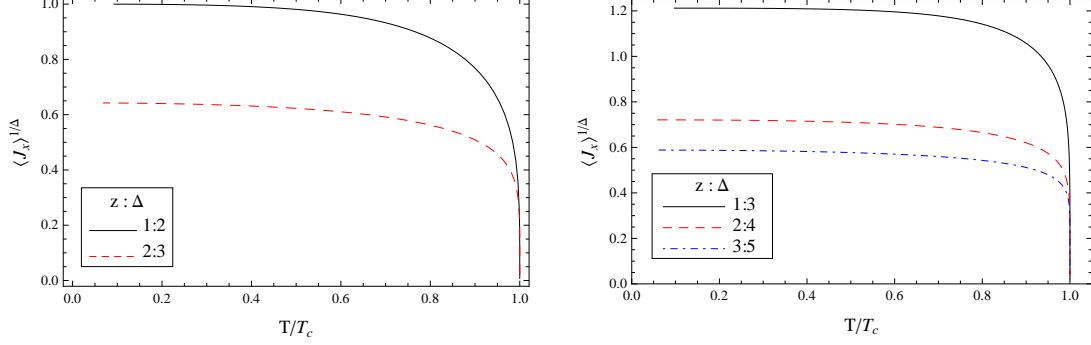


FIG. 6: The condensation versus temperature of the p wave models in $D = 4$ (left) and $D = 5$ (right). Curves from top to bottom correspond to $z = 1$ (solid), 2 (dashed), 3 (dotted), respectively. The notation $z : d = 1 : 2$ denotes that $z = 1$ and $d = 2$.

The condensation of vector field specifies the x direction, so the conductivity along the x direction σ_{xx} is expected to be different from that along the y direction σ_{yy} . To calculate the conductivity, we turn on the perturbation [6]

$$\delta A = e^{-i\omega t} (a_t^1 \tau^1 dt + a_t^2 \tau^2 dt + a_x^3 \tau^3 dx + a_y^3 \tau^3 dy). \quad (52)$$

The linearized Yang-Mills equations of motion result in four second order equations

$$a_y^{3''} + \left(\frac{d+z-1}{r} + \frac{f'}{f} \right) a_y^{3'} + \frac{\omega^2}{r^{2z+2} f^2} a_y^3 - \frac{\psi^2}{r^4 f} a_y^3 = 0, \quad (53)$$

$$a_t^{1''} + \frac{d-z+1}{r} a_t^{1'} + \frac{\psi \phi}{r^4 f} a_x^3 = 0,$$

$$a_t^{2''} + \frac{d-z+1}{r} a_t^{2'} - \frac{\psi}{r^4 f} (i\omega a_x^3 + \psi a_t^2) = 0, \quad (54)$$

$$a_x^{3''} + \left(\frac{d+z-1}{r} + \frac{f'}{f} \right) a_x^{3'} - \frac{1}{r^{2z+2} f^2} (-\omega^2 a_x^3 + i\omega \psi a_t^2 + \psi \phi a_t^1) = 0,$$

and two first order constraints

$$i\omega a_t^{1'} - \phi' a_t^2 + \phi a_t^{2'} = 0, \quad (55)$$

$$i\omega a_t^{2'} + \phi' a_t^1 - \phi a_t^{1'} + r^{2z-2} f (\psi' a_x^3 - \psi a_x^{3'}) = 0. \quad (56)$$

Obviously, a_y^3 is independent of other components, while a_x^1 mixes with a_t^1 and a_t^2 . We impose the ingoing wave conditions near the horizon

$$a_y^3(r) = (r - r_+)^{-i\omega/4\pi T} (1 + a_{y31}(r - r_+) + a_{y32}(r - r_+)^2 + a_{y33}(r - r_+)^3 + \dots), \quad (57)$$

$$a_t^1(r) = (r - r_+)^{-i\omega/4\pi T} (a_{t11}(r - r_+) + a_{t12}(r - r_+)^2 + a_{t13}(r - r_+)^3 + \dots),$$

$$a_t^2(r) = (r - r_+)^{-i\omega/4\pi T} (a_{t21}(r - r_+) + a_{t22}(r - r_+)^2 + a_{t23}(r - r_+)^3 + \dots), \quad (58)$$

$$a_x^3(r) = (r - r_+)^{-i\omega/4\pi T} (1 + a_{x31}(r - r_+) + a_{x32}(r - r_+)^2 + a_{x33}(r - r_+)^3 + \dots).$$

TABLE III: The asymptotical solutions of p wave models in Lifshitz black holes, where $i = 1, 2, \mu = x, y$ and ξ is a constant.

	$d = 3, z = 1$	$d = 3, z = 2$	$d = 3, z = 3$	$d = 2, z = 1$	$d = 2, z = 2$
$a_t^i(r)$	$a_t^{i(0)} + \frac{a_t^{i(2)}}{r^2}$	$a_t^{i(0)} + \frac{a_t^{i(1)}}{r}$	$a_t^{i(0)} + a_t^{i(1)} \ln \xi r$	$a_t^{i(0)} + \frac{a_t^{i(1)}}{r}$	$a_t^{i(0)} + a_t^{i(1)} \ln \xi r$
$a_\mu^3(r)$	$a_\mu^{3(0)} + \frac{a_\mu^{3(2)}}{r^2} + \frac{a_\mu^{3(0)} \omega^2}{2r^2} \ln \xi r$	$a_\mu^{3(0)} + \frac{a_\mu^{3(3)}}{r^3}$	$a_\mu^{3(0)} + \frac{a_\mu^{3(4)}}{r^4}$	$a_\mu^{3(0)} + \frac{a_\mu^{3(1)}}{r}$	$a_\mu^{3(0)} + \frac{a_\mu^{3(2)}}{r^2}$

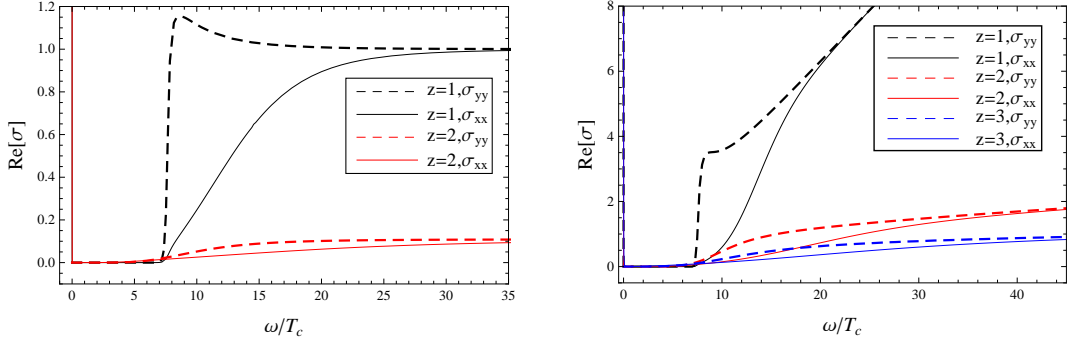


FIG. 7: The real part of the AC conductivity versus frequency of a_y^3 (dashed) and a_x^3 (solid) at $T/T_c \approx 0.1$ in 4 (left), 5 (right) dimensional black holes. From top to bottom, both solid and dashed curves correspond to $z = 1, 2$ in $D = 4$ and $z = 1, 2, 3$ in $D = 5$, respectively.

Near the boundary, the general expansions are listed in Tab. III, where we only show the leading order term and the sub-leading order term. As noticed in Ref. [6], there exist two gauge freedoms for a_x^3 , which are fixed by choosing the axial gauge along the r direction and constructing the gauge invariant quantity

$$\hat{a}_x^3 = a_x^3 + \psi \frac{i\omega a_t^2 + \phi a_t^1}{\phi^2 - \omega^2}. \quad (59)$$

Expanding \hat{a}_x^3 near the boundary, σ_{xx} can be expressed by the leading order term $\hat{a}_x^{3(0)}$ and the coefficient of the sub-leading order term $\hat{a}_x^{3(1)}$ as

$$\sigma_{xx}(\omega) = \frac{\hat{a}_x^{3(1)}}{i\omega \hat{a}_x^{3(0)}}, \quad (60)$$

while σ_{yy} is similar to the formula (16), where the logarithmic divergence term can be removed by the holographic renormalization. The conductivity σ_{yy} and σ_{xx} with various z in $D = 4$ (5) are plotted in Figs. 7, 8 and 9.

Figure 7 exhibits the real part of conductivity, from which we can find that when $z = 1$, there is an obvious energy gap parameterized by ω_g for $Re[\sigma_{yy}]$, while the gap of $Re[\sigma_{xx}]$ behaves rather softer. Especially, the result corresponding to $z = 1$ in $D = 4$ can reduce to that in Ref. [6]. When $z = 2$ (3), the curves for $Re[\sigma_{yy}]$ and $Re[\sigma_{xx}]$ become flatter than the case of $z = 1$ and the

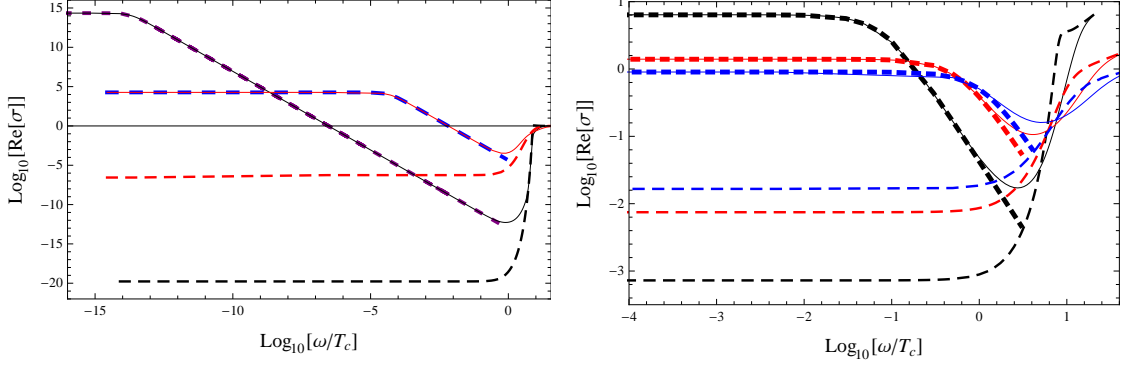


FIG. 8: The real part of the AC conductivity versus frequency of a_y^3 (dashed) and a_x^3 (solid) in 4 (left, $T/T_c \approx 0.1$), 5 (right, $T/T_c \approx 0.5$) dimensional black holes. From top (bottom) to bottom (top), the solid (dashed) curves correspond to $z = 1, 2$ in $D = 4$ and $z = 1, 2, 3$ in $D = 5$, respectively. The dashed lines along $Re[\sigma_{xx}]$ are the best fits of the Drude model prediction.

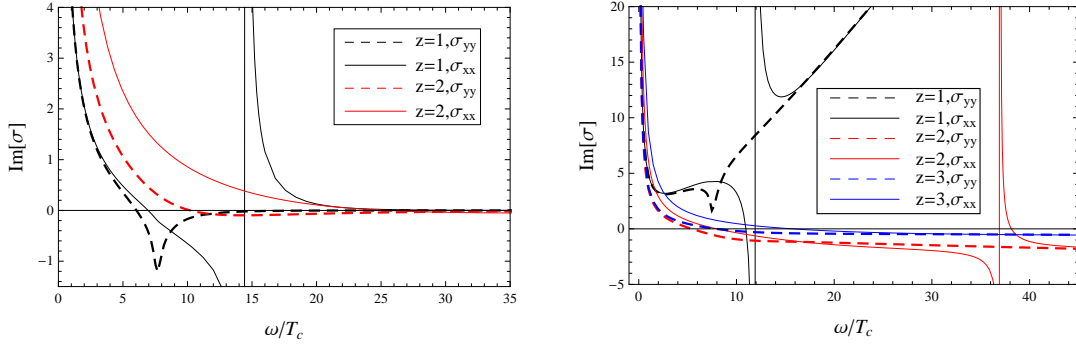


FIG. 9: The imaginary part of the AC conductivity versus frequency of a_y^3 (dashed) and a_x^3 (solid) at $T/T_c \approx 0.1$ in the 4 (left), 5 (right) dimensional black holes with $z = 1$ (black), 2 (red), 3 (blue).

difference between $Re[\sigma_{xx}]$ and $Re[\sigma_{yy}]$ also decreases. Since the difference between $Re[\sigma_{yy}]$ and $Re[\sigma_{xx}]$ just exhibits the anisotropy of conductivity, the larger z might suppress the anisotropy of the system. The results with $z = 2$ in $D = 4$ are consistent with ones in Ref. [35]. To show the behavior of conductivity at low frequency limit, we plot the logarithmic behavior of conductivity in Fig. 8, from which we can obtain that the difference between $Re[\sigma_{xx}]$ and $Re[\sigma_{yy}]$ decreases when we increase z ($z = 1, 2$ in $D = 4$ and $z = 1, 2, 3$ in $D = 5$). Figure 9 shows the imaginary part of conductivity, from which we conclude in various cases, there is a pole at $\omega = 0$, which means the DC superconductivity. In the intermediate region, for a_y^3 , the minimum of $Im[\sigma]$ exactly corresponds to the location of the gap of $Re[\sigma]$ for $z = 1$. However, this gap vanishes in $z = 2$ and $z = 3$ cases.

In addition, we display the superfluid density n_s^y (n_s^x) for a_y^3 (a_x^3) in the left plot of Fig. 10 and also fit the mass of quasiparticles $\tilde{\Delta}$ as well as the Drude peak $Re[\sigma]_{Drude} = \frac{\sigma_0}{1+\omega^2\tau^2}$, where σ_0 is a constant related to the density of charge carriers and τ is the scattering time. The related results

TABLE IV: The numerical results of the p wave superconductors in the black holes when $D = 4$ (5), where $t = 1 - T/T_c$, $\tilde{t} = 1 - (T/T_c)^{1/2}$.

D	z	Δ	$T_c/\rho^{z/d}$	$\langle J_x \rangle^{1/\Delta}(T \approx T_c)$	$n_s^y(T \approx T_c)$	$n_s^x(T \approx T_c)$	$\tilde{\Delta}$	σ_0	τ
4	1	2	0.125	$1.40t^{1/2\Delta}$	$3.19t$	$1.04t$	0.62	2.65×10^{13}	4.03×10^{14}
4	2	3	0.037	$0.76t^{1/2\Delta}$	$0.93t$	$0.85t$	0.04	684.50	559459
5	1	3	0.201	$1.62t^{1/2\Delta}$	$4.75t$	$2.37t$	1.20	1.28	60.85
5	2	4	0.065	$0.92\tilde{t}^{1/2\Delta}$	$0.91t$	$0.90t$	0.08	0.09	24.92
5	3	5	0.020	$0.60t^{1/2\Delta}$	$0.22t$	$0.36t$	0.01	0.02	44.50

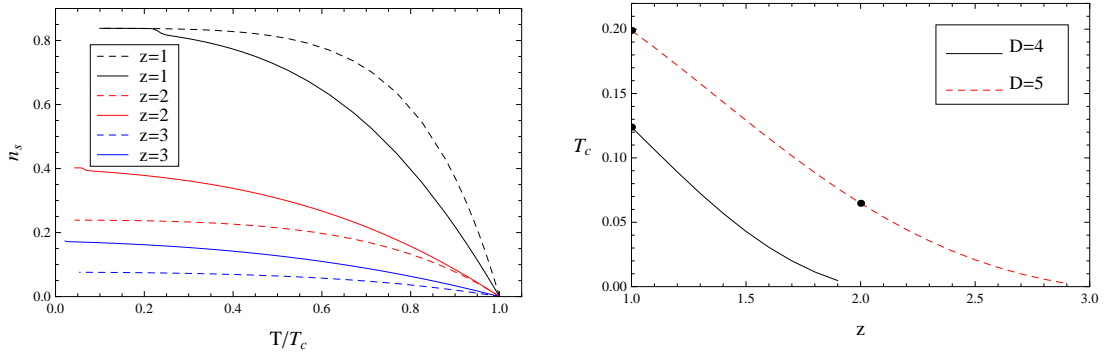


FIG. 10: The superfluid density versus temperature (left) and the analytical T_c versus z (right) of p wave models. Curves (left plot) of a_x^3 (solid) and a_y^3 (dashed) correspond to $z = 1, 2, 3$ (from top to bottom) in $D = 5$, respectively. Curves (right plot) correspond to $D = 4$ (bottom) and $D = 5$ (top), respectively.

are listed in Tab. IV, from which we find as z increases ($z = 1, 2$ in $D = 4$ and $z = 1, 2, 3$ in $D = 5$), all quantities in the table decrease except τ . Especially, n_s^y (n_s^x) decreases with $(1 - T/T_c)$ linearly near T_c . n_s^y (n_s^x) in $D = 4$ is similar to the one in $D = 5$.

Next we study the p wave model analytically. The gauge field $\phi(u)$ obeys the form (19), while the condensed field takes

$$\psi(u) = \frac{\langle J_x \rangle}{r_+^{d+z-2}} u^{d+z-2} F(u), \quad (61)$$

where $F = 1 - \alpha u^2$, so we can deduce Eq. (49) to the eigenvalue equation (21) with coefficients

$$\mathcal{T} = u^{d+z-1} (1 - u^{d+z}), \mathcal{P} = (d+z)(d+z-2)u^{2d+2z-3}, \mathcal{Q} = -\frac{u^{d+z-3} (u^d - u^z)^2}{u^{d+z} - 1}. \quad (62)$$

According to Eq. (24), the critical temperature versus arbitrary $z \in [1, d]$ is shown in the right plot of Fig. 10. It follows that T_c decreases smoothly when z increases, which indicates that the increasing z inhibits the superconductor phase transition. We read off the analytical T_c of some

special points

$$\begin{aligned}
\alpha &= 0.5077, \lambda^2 = 13.767, T_c = 0.124\rho^{1/2}, \quad \text{for } z = 1, D = 4, \\
\alpha &= 0.6851, \lambda^2 = 16.745, T_c = 0.199\rho^{1/3}, \quad \text{for } z = 1, D = 5, \\
\alpha &= 0.7421, \lambda^2 = 232.229, T_c = 0.065\rho^{2/3}, \quad \text{for } z = 2, D = 5,
\end{aligned} \tag{63}$$

which is consistent with the numerical result listed in Tab. IV. Especially, the result corresponding to $z = 1$ in $D = 4$ can restore to the case in Ref. [6].

In addition, we find the behavior of condensation of the p wave model also has the form (29). Some concrete results yield

$$\langle J_x \rangle^{\frac{1}{2}}|_{d=2, z=1} = 1.34 \left(1 - \frac{T}{T_c}\right)^{\frac{1}{4}}, \langle J_x \rangle^{\frac{1}{3}}|_{d=3, z=1} = 2.58 \left(1 - \frac{T}{T_c}\right)^{\frac{1}{6}}, \langle J_x \rangle^{\frac{1}{4}}|_{d=3, z=2} = 0.50 \left(1 - \left(\frac{T}{T_c}\right)^{\frac{1}{2}}\right)^{\frac{1}{8}}, \tag{64}$$

which agrees with the above numerical results at the same order.

B. p wave superconductors in Lifshitz solitons

Following Ref. [18], in this subsection we generalize the p wave superconductor model to the Lifshitz soliton background. Equations of motion in terms of $\psi(r)$ and $\phi(r)$ obey

$$\psi'' + \left(\frac{d+z-1}{r} + \frac{f'}{f}\right) \psi' + \frac{\phi^2}{r^4 f} \psi = 0, \tag{65}$$

$$\phi'' + \left(\frac{d+z-1}{r} + \frac{f'}{f}\right) \phi' - \frac{\psi^2}{r^4 f} \phi = 0, \tag{66}$$

which suggest that the behavior of superconductors is determined by the parameter $(d+z)$. The boundary conditions of $\psi(r)$ and $\phi(r)$ at the tip $r = r_0$ are the same with the case in s wave model. Near the boundary, the general solution of $\psi(r)$ has the form (51), while $\phi(r)$ takes the form (33).

The condensation $\langle J_x \rangle$ and the charge density ρ in $D = 5$ are plotted in Fig. 11, while μ_c and related coefficients are listed in Tab. VI, from which we can see when z increases ($z = 1, 2, 3$), μ_c increases. When μ is slightly beyond μ_c , $\rho = C_\rho(\mu - \mu_c)$ and $\langle \mathcal{O} \rangle = C_{\mathcal{O}}\sqrt{\mu - \mu_c}$, which is consistent with the results in the mean field theory. For $z = 1$ in $D = 5$, the results can restore to ones in Refs. [15, 18, 19].

In the presence of the condensation $\psi\tau^1 dx$, the perturbation along the x direction is expected to be mixed with other components. To calculate the conductivity along the x direction σ_{xx} , we should turn on as many as components. Considering the axial gauge $A_r^a = 0$, we turn on the general perturbations in $D = 5$

$$\delta A = e^{-i\omega t} a_\mu^a \tau^a dx^\mu, \quad a = 1, 2, 3, \mu = t, x, y, \chi. \tag{67}$$

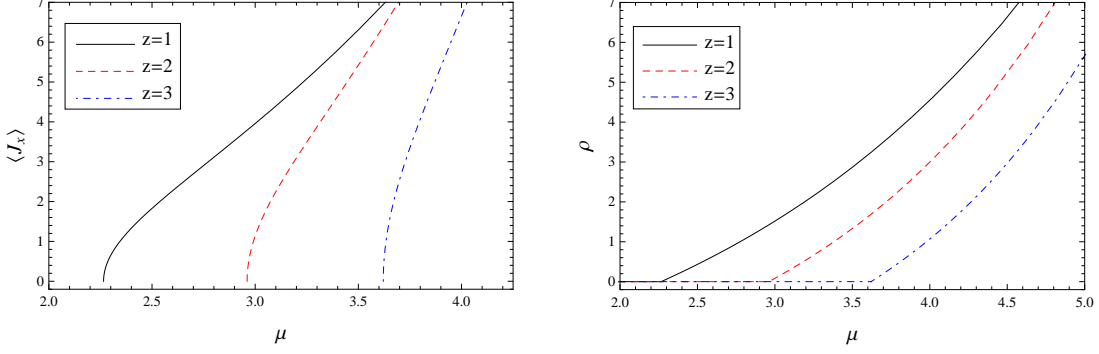


FIG. 11: The condensation (left) and the charge density (right) versus chemical potential of the p wave model in 5 dimensional solitons with $z = 1, 2, 3$ (from left to right).

TABLE V: The asymptotical solutions of the perturbation of a_y^3 and a_x^3 in 4 (5) dimensional solitons, where $\mu = x, y$ in $d = 3$ and x in $d = 2$, and $i = 1, 2$.

	$d = 3(2), z = 1(2)$	$d = 3(2), z = 2(3)$	$d = 3, z = 3$	$d = 2, z = 1$
$a_t^i(r)$	$a_t^{i(0)} + \frac{a_t^{i(2)}}{r^2}$	$a_t^{i(0)} + \frac{a_t^{i(3)}}{r^3}$	$a_t^{i(0)} + \frac{a_t^{i(4)}}{r^4}$	$a_t^{i(0)} + \frac{a_t^{i(1)}}{r}$
$a_\mu^3(r)$	$a_\mu^{3(0)} + \frac{a_\mu^{3(2)}}{r^2} + \frac{a_\mu^{3(0)}\omega^2}{2r^2} \ln \xi r$	$a_\mu^{3(0)} + \frac{a_\mu^{3(0)}\omega^2}{2r^2} + \frac{a_\mu^{3(3)}}{r^3}$	$a_\mu^{3(0)} + \frac{a_\mu^{3(0)}\omega^2}{4r^2} + \frac{a_\mu^{3(4)}}{r^4} + \frac{a_\mu^{3(0)}\omega^4}{16r^4} \ln \xi r$	$a_\mu^{3(0)} + \frac{a_\mu^{3(1)}}{r}$

The above ansatz with $a_y^a = 0$ turns into that of the case of $D = 4$. The linearized Yang-Mills equations read a independent equation about a_y^3 (only in $D = 5$)

$$a_y^{3''} + \left(\frac{f'}{f} + \frac{d+z-1}{r} \right) a_y^{3'} + \frac{\omega^2}{r^4 f} a_y^3 - \frac{\psi^2}{r^4 f} a_y^3 = 0, \quad (68)$$

and three equations about a_x^3 (in $D = 4, 5$)

$$\begin{aligned} a_t^{1''} + \left(\frac{f'}{f} + \frac{d+z-1}{r} \right) a_t^{1'} + \frac{\psi\phi}{r^4 f} a_x^3 &= 0, \\ a_t^{2''} + \left(\frac{f'}{f} + \frac{d+z-1}{r} \right) a_t^{2'} - \frac{\psi(a_t^2\psi + i\omega a_x^3)}{r^4 f} &= 0, \\ a_x^{3''} + \left(\frac{f'}{f} + \frac{d+z-1}{r} \right) a_x^{3'} + \frac{\omega^2 a_x^3 - i\omega a_t^2\psi - a_t^1\psi\phi}{r^4 f} &= 0, \end{aligned} \quad (69)$$

as well as two constraints

$$i\omega a_t^{1'} - \phi' a_t^2 + \phi a_t^{2'} = 0, \quad (70)$$

$$i\omega a_t^{2'} + \phi' a_t^1 - \phi a_t^{1'} + \psi' a_x^3 - \psi a_x^{3'} = 0. \quad (71)$$

Obviously, the other components decouple from a_y^3 , a_t^1 , a_t^2 and a_x^3 . Boundary conditions of the above components at the tip are similar to the formula (35). Near the boundary, general falloffs are listed in Tab. V, where we only list the leading order and the sub-leading order terms.

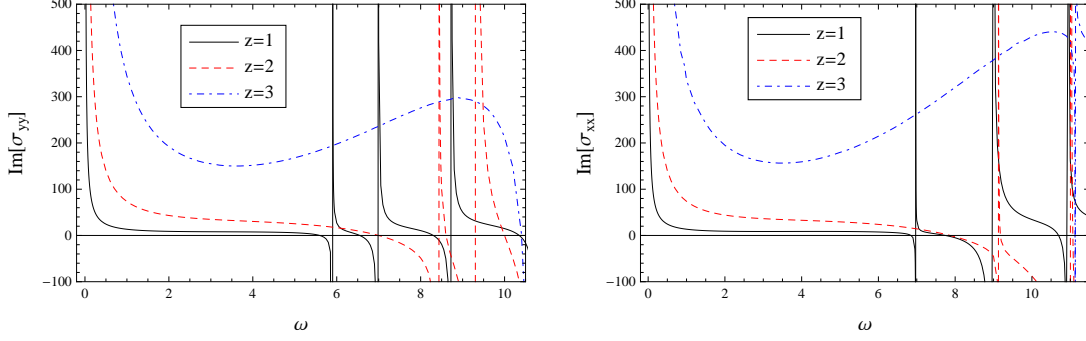


FIG. 12: The imaginary part of the conductivity versus frequency of a_y^3 (left) and a_x^3 (right) at $\mu/\mu_c \approx 4$ in the 5 dimensional solitons with $z = 1, 2, 3$ (from left to right).

TABLE VI: Results of the p wave models in $D = 4$ (5), where $t = (\mu - \mu_c)^{1/2}$ and quantities $\langle J_x \rangle$, $\langle J_x \rangle_{SL}$, ρ , ρ_{SL} , n_s^x and n_s^y are all calculated near μ_c .

D	z	μ_c	$\langle J_x \rangle$	ρ	n_s^y	ω_n^y	ω_s^y	n_s^x	ω_n^x	ω_s^x	$\mu_{c;SL}$	$\langle J_x \rangle_{SL}$	ρ_{SL}
4	1	1.491	$1.90t$	$1.40t^2$	–	–	–	$0.63t^2$	1.49	4.96	1.491	$1.59t$	$1.04t^2$
4	2	2.265	$3.45t$	$1.76t^2$	–	–	–	$0.69t^2$	2.26	6.98	2.267	$2.56t$	$1.13t^2$
4	3	2.961	$5.62t$	$2.10t^2$	–	–	–	$0.72t^2$	2.90	9.16	2.965	$3.73t$	$1.22t^2$
5	1	2.265	$3.45t$	$1.76t^2$	$0.69t^2$	2.27	5.90	$0.69t^2$	2.27	6.97	2.267	$2.56t$	$1.13t^2$
5	2	2.961	$5.62t$	$2.12t^2$	$0.73t^2$	2.97	8.43	$0.73t^2$	2.97	9.13	2.965	$3.73t$	$1.22t^2$
5	3	3.621	$8.66t$	$2.49t^2$	$0.76t^2$	3.63	10.64	$0.76t^2$	3.63	10.64	3.630	$5.12t$	$1.32t^2$

As a typical example, for a_y^3 (a_x^3), we plot the conductivity in $D = 5$ in Fig. 12, while the superfluid density n_s^y (n_s^x) and the second pole of the conductivity in normal phase ω_n^y (ω_n^x) in $D = 4$ (5) are given in Tab. VI, from which we can obtain following results.

- (1) All quantities in the table increase when z increases ($z = 1, 2, 3$). In the normal phase, σ_{xx} overlaps σ_{yy} . What is more, the value of ω_n^y (ω_n^x) is basically equal to μ_c numerically, which does not occur in the s wave model.
- (2) The location of the second pole of $Im[\sigma]$ for a_y^3 (a_x^3) in the superconducting phase ω_s^y (ω_s^x) moves right by comparing with ω_n^y (ω_n^x). The location of ω_s^x is larger than the one of ω_s^y in $D = 5$, which suggests the anisotropy of the conductivity. The difference between ω_s^x and ω_s^y decreases when z increases ($z = 2$ and $z = 3$), which perhaps suggests that the anisotropy of conductivity is suppressed with the increasing z .
- (3) In the case of $z = 3$ in $D = 5$, the monotonicity of $Im[\sigma(\omega)]$ breaks, which also appears in the s wave case. It indicates that z indeed changes the behavior of our holographic model.

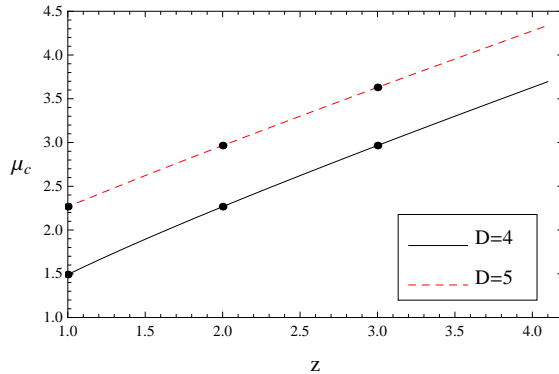


FIG. 13: The z dependent μ_c of the p wave models in the 4 (bottom), 5 (top) dimensional solitons.

Following the analytical procedure of the s wave model, we obtain the coefficients of the SL eigenvalue equation (38) for the p wave model in $D = 5$

$$\mathcal{T} = u^{z+2} (1 - u^{z+3}), \quad \mathcal{P} = (z^2 + 4z + 3) u^{2z+3}, \quad \mathcal{Q} = u^{z+2}. \quad (72)$$

The critical chemical potential versus arbitrary $z \geq 1$ in $D = 4$ (5) is plotted in Fig. 13, from which we find that μ_c increases with the increase of z smoothly. In addition, some special analytic results are listed in Tab. VI. Evidently, the analytical μ_c is consistent with the numerical result, while the analytical results of the condensation and the charge density match the numerical results at the same order. Especially, the results with $z = 1$ in $D = 5$ can reduce to ones in Refs. [14, 16, 18].

IV. CONCLUSION AND DISCUSSION

In this paper, we have studied holographic superconductors in both (3+1) and (4+1) dimensional Lifshitz spacetimes in the probe limit numerically and analytically. The effects of the anisotropy of the spacetime on the superconductors are investigated. Main results are listed as follows.

- (1) In the black hole backgrounds, for both the s wave and p wave models, when z increases ($z = 1, 2$ in $D = 4$ and $1, 2, 3$ in $D = 5$), the critical temperature decreases, which suggests that the phase transition becomes more difficult with the increasing z . Near T_c , both $\langle \mathcal{O} \rangle$ and $\langle J_x \rangle$ behave as $\sim (1 - (T/T_c)^{d/z})^{1/2}$ with general z and $D = d + 2$, which looks different from the standard form $\sim (1 - T/T_c)^{1/2}$. This results from the Lifshitz scaling dimension. It is in this sense we say the critical exponent for the condensation is still $1/2$. In addition, for the p wave models, the increasing z seems to suppress the anisotropy between σ_{yy} and σ_{xx} .

- (2) In the soliton backgrounds, when z increases ($z = 1, 2, 3$), μ_c decreases in the s wave models but increases in the p wave cases. Near μ_c , the system undergoes a second order phase transition. For both two models, as z increases, the location of the second pole of $Im[\sigma]$ in the normal phase ω_n (ω_n^y, ω_n^x) increases, while that in the superconducting phase ω_s (ω_s^y, ω_s^x) moves right by comparing with ω_n (ω_n^y, ω_n^x). The value of ω_n^y (ω_n^x) is basically equal to μ_c in the p wave model. The difference between σ_{xx} and σ_{yy} decreases with the increase of z ($z = 1, 2, 3$), which implies that the increasing z suppresses the anisotropy of the system.
- (3) For both the black hole and soliton cases, the analytical results uphold the numerical ones, especially for the critical temperature T_c (μ_c).

In this paper we have solved the coupled equations of motion with integral z numerically. In principle, our calculations can be extended to the general cases with $z \geq 1$. Furthermore, we have only worked on the probe limit by neglecting the back reaction of the matter fields. It has been shown that new phases can emerge (see Refs. [39, 40] for example) and the order of the phase transition can be also changed [41, 42] once taking the back reaction into consideration. Therefore, it is interesting to study the back reaction of the matter field to the Lifshitz background and to see some new features by comparing with the results in the probe limit.

Acknowledgments

We would like to thank S. A. Hartnoll for his help about the numerical code. We also would like to take this opportunity to extremely thank R. G. Cai for his directive help and support. One of the authors (J. W. Lu) is deeply grateful to L. Li, Y. Y. Bu and M. L. Liu for their helpful discussions and comments, especially thank L. Li for everything. This work is supported by the National Natural Science Foundation of China (Grant No. 11175077), the Natural Science Foundation of Liaoning Province (Grant No. L2011189) and the PhD Programs of Ministry of China (Grant No. 20122136110002).

-
- [1] J. M. Maldacena, The large-N limit of superconformal field theories and supergravity, *Adv. Theor. Math. Phys.* **2**, 231 (1998) [arXiv:hep-th/9711200].
- [2] S. A. Hartnoll, C. P. Herzog, and G. T. Horowitz, Building a Holographic Superconductor, *Phys. Rev. Lett.* **101**, 031601 (2008) [arXiv:0803.3295].

- [3] G. T. Horowitz and M. M. Roberts, Holographic superconductors with various condensates, Phys. Rev. D **78**, 126008 (2008) [arXiv:0810.1077].
- [4] G. T. Horowitz and M. M. Roberts, Zero temperature limit of holographic superconductors, JHEP **11**, 015 (2009) [arXiv:0908.3677].
- [5] G. Siopsis and J. Therrien, Analytic calculation of properties of holographic superconductors, JHEP **05**, 013 (2010) [arXiv:1003.4275].
- [6] S. S. Gubser and S. S. Pufu, The gravity dual of a p wave superconductor, JHEP **11**, 033 (2008) [arXiv:0805.2960].
- [7] R. G. Cai, S. He, L. Li, and L. F. Li, A Holographic Study on Vector Condensate Induced by a Magnetic Field, [arXiv:1309.2098].
- [8] R. G. Cai, L. Li, and L. F. Li, A Holographic P-wave Superconductor Model, [arXiv:1309.4877].
- [9] F. Aprile, D. Rodriguez-Gomez, and J. G. Russo, p-wave Holographic Superconductors and five-dimensional gauged Supergravity, JHEP **01**, 056 (2011) [arXiv:1011.2172].
- [10] J. W. Chen, Y. J. Kao, D. Maity, W. Y. Wen, and C. P. Yeh, Towards a holographic model of D -wave superconductors, Phys. Rev. D **81**, 106008 (2010) [arXiv:1003.2991].
- [11] F. Benini, C. P. Herzog, R. Rahman, and A. Yarom, Gauge gravity duality for d-wave superconductors: prospects and challenges, JHEP **11**, 137 (2010) [arXiv:1007.1981].
- [12] K. Y. Kim and M. Taylor, Holographic d-wave superconductors, JHEP **08**, 112 (2013) [arXiv:1304.6729].
- [13] T. Nishioka, S. Ryu, and T. Takayanagi, Holographic Superconductor/Insulator Transition at Zero Temperature, JHEP **03**, 131 (2010) [arXiv:0911.0962].
- [14] H. F. Li, Further studies on holographic insulator/superconductor phase transitions from Sturm-Liouville eigenvalue problems, JHEP **07**, 135 (2013) [arXiv:1306.3071].
- [15] R. G. Cai, X. He, H. F. Li, and H. Q. Zhang, Phase transitions in AdS soliton spacetime through marginally stable modes, Phys. Rev. D **84**, 046001 (2011) [arXiv:1105.5000].
- [16] R. G. Cai, H. F. Li, and H. Q. Zhang, Analytical studies on holographic insulator/superconductor phase transitions, Phys. Rev. D **83**, 126007 (2011) [arXiv:1103.5568].
- [17] Q. Y. Pan, J. L. Jing, and B. Wang, Analytical investigation of the phase transition between holographic insulator and superconductor in Gauss-Bonnet gravity, JHEP **11**, 088 (2011) [arXiv:1105.6153].
- [18] A. Akhavan and M. Alishahiha, P-wave holographic insulator/superconductor phase transition, Phys. Rev. D **83**, 086003 (2011) [arXiv:1011.6158].
- [19] R. G. Cai, L. Li, L. F. Li and R. K. Su, Entanglement Entropy in Holographic P-Wave Superconductor/Insulator Model, [arXiv:1303.4828].
- [20] S. Kachru, X. Liu, and M. Mulligan, Gravity duals of Lifshitz-like fixed points, Phys. Rev. D **78**, 106005 (2008) [arXiv:0808.1725].
- [21] M. Taylor, Non-relativistic holography, [arXiv:0812.0530].
- [22] D. W. Pang, A Note on Black Holes in Asymptotically Lifshitz Spacetime, [arXiv:0905.2678].
- [23] K. Balasubramanian and J. McGreevy, An analytic Lifshitz black hole, Phys. Rev. D **80**, 104039 (2009)

- [arXiv:0909.0263].
- [24] G. Bertoldi, B. A. Burrington, and A. Peet, Black holes in asymptotically Lifshitz spacetimes with arbitrary critical exponent, *Phys. Rev. D* **80**, 126003 (2009)[arXiv:0905.3183].
- [25] R. G. Cai, Y. Liu, and Y. W. Sun, A Lifshitz black hole in four dimensional R^2 gravity, *JHEP* **10**, 080 (2009) [arXiv:0909.2807].
- [26] J. Gath, J. Hartong, R. Monteiro, and N. A. Obers, Holographic Models for Theories with Hyperscaling Violation, *JHEP* **04**, 159 (2013) [arXiv:1212.3263].
- [27] E. J. Brynjolfsson, U. H. Danielsson, L. Thorlacius, and T. Zingg, Holographic superconductors with Lifshitz scaling, *J. Phys. A: Math. Theor.* **43**, 065401 (2010) [arXiv:0908.2611].
- [28] S. J. Sin, S. S. Xu, and Y. Zhou, holographic superconductor for a lifshitz fixed point, *Int. J. Mod. Phys. A* **26**, 4617 (2011) [arXiv:0909.4857].
- [29] S. A. Hartnoll, J. Polchinski, E. Silverstein, and D. Tong, Towards strange metallic holography, *JHEP* **04**, 120 (2010) [arXiv:0912.1061].
- [30] J. R. Sun, S. Y. Wu, and H. Q. Zhang, Novel Features of the Transport Coefficients in Lifshitz Black Branes, *Phys. Rev. D* **87**, 086005 [arXiv:1302.5309].
- [31] Z. Y. Fan, Holographic superconductors with hyperscaling violation, [arXiv:1305.2000].
- [32] E. Abdalla, J. d. Oliveira, A. B. Pavan, and C. E. Pellicer, Holographic phase transition and conductivity in three dimensional Lifshitz black hole, [arXiv:1307.1460].
- [33] D. W. Pang, Conductivity and Diffusion Constant in Lifshitz Backgrounds, *JHEP* **01**, 120 (2010) [arXiv:0912.2403].
- [34] C. Park, Notes on the holographic Lifshitz theory, [arXiv:1305.6690].
- [35] Y. Y. Bu, Holographic superconductors with $z = 2$ Lifshitz scaling, *Phys. Rev. D* **86**, 046007 (2012) [arXiv:1211.0037].
- [36] Y. S. Myung and T. Moon, Quasinormal frequencies and thermodynamic quantities for the Lifshitz black holes, *Phys. Rev. D* **86**, 024006 (2012) [arXiv:1204.2116].
- [37] B. Way, Holographic confinement/deconfinement transitions in asymptotically Lifshitz spacetimes, *Phys. Rev. D* **86**, 086007 (2012) [arXiv:1207.4205].
- [38] R. G. Cai and H. Q. Zhang, Holographic superconductors with Hořava-Lifshitz black holes, *Phys. Rev. D* **81**, 066003 (2010) [arXiv:0911.4867].
- [39] R. G. Cai, L. Li, L. F. Li, and Y. Q. Wang, Competition and Coexistence of Order Parameters in Holographic Multi-Band Superconductors, [arXiv:1307.2768].
- [40] Y. Liu, K. Schalm, Y. W. Sun, and J. Zaanen, Bose-Fermi competition in holographic metals, [arXiv:1307.4572].
- [41] G. T. Horowitz and B. Way, Complete Phase Diagrams for a Holographic Superconductor/Insulator System, *JHEP* **11**, 011 (2010) [arXiv:1007.3714].
- [42] R. G. Cai, S. He, L. Li, and L. F. Li, Entanglement Entropy and Wilson Loop in Stüeckelberg Holographic Insulator/Superconductor Model, *JHEP* **10**, 107 (2012) [arXiv:1209.1019].